

# Model independent constraints on contact interactions from polarized Bhabha scattering at LC.

A. Pankov<sup>a,b</sup> and N. Paver<sup>a</sup>

<sup>a</sup> Dipartimento di Fisica Teorica, Università di Trieste and  
Istituto Nazionale di Fisica Nucleare, Sezione di Trieste, Trieste, Italy

<sup>b</sup> The Abdus Salam International Centre for Theoretical Physics, Trieste, Italy

## Abstract

We discuss electron-electron contact-interaction searches in the process  $e^+e^- \rightarrow e^+e^-$  at a future  $e^+e^-$  Linear Collider with c.m. energy  $\sqrt{s} = 0.5$  TeV and with both beams longitudinally polarized. Our analysis is based on the measurement of the polarized differential cross sections, and allows to simultaneously take into account the general set of contact interaction couplings as independent, non-zero, parameters thus avoiding simplifying, model-dependent, assumptions. We evaluate the corresponding model-independent constraints on the coupling constants, emphasizing the role of beam polarization, and make a comparison with the case of  $e^+e^- \rightarrow \mu^+\mu^-$ .

# 1 Introduction

Contact interaction Lagrangians (CI) provide an effective framework to account for the phenomenological effects of new dynamics characterized by extremely high intrinsic mass scales  $\Lambda$ , at the ‘low’ energies  $\sqrt{s} \ll \Lambda$  attainable at current particle accelerators. Typically, ‘low energy’ manifestations of quark and lepton substructure would occur *via* four-fermion quark and lepton contact interactions, induced by exchanges of very heavy sub-constituent bound states with mass of the order of  $\Lambda$  [1]. However, this concept is quite general, and is adequate to the description of a wide class of quark and lepton cross sections governed by exchanges of objects associated to new gauge interactions such as, *e.g.*, heavy neutral gauge bosons and leptoquarks, in a regime where such masses are much larger than the Mandelstam variables of the process.

The explicit parameterization of the four-fermion quark and lepton contact interactions is, *a priori*, somewhat arbitrary. In general, it must respect  $SU(3) \times SU(2) \times U(1)$  symmetry, because the new dynamics are active well-beyond the electroweak scale. Furthermore, usually one limits to the lowest dimensional operators,  $D = 6$  being the minimum, and neglects higher dimensional operators that are suppressed by higher powers of  $1/\Lambda^2$  and therefore are expected to give negligible effects.

In this note, we consider the effects of the flavor-diagonal, helicity conserving, *eeff* contact-interaction effective Lagrangian [2]

$$\mathcal{L}_{\text{CI}} = \frac{1}{1 + \delta_{ef}} \sum_{i,j} g_{\text{eff}}^2 \epsilon_{ij} (\bar{e}_i \gamma_\mu e_i) (\bar{f}_j \gamma^\mu f_j), \quad (1)$$

in the Bhabha scattering process

$$e^+ + e^- \rightarrow e^+ + e^- \quad (2)$$

at an  $e^+e^-$  Linear Collider (LC) with c.m. energy  $\sqrt{s} = 0.5 \text{ TeV}$  and polarized electron and positron beams. In Eq. (1):  $i, j = \text{L, R}$  denote left- or right-handed fermion helicities,  $f$  indicates the fermion species, so that  $\delta_{ef} = 1$  for the process (2) under consideration, and the CI coupling constants are parameterized in terms of corresponding mass scales as  $\epsilon_{ij} = \eta_{ij}/\Lambda_{ij}^2$ . Actually, one assumes  $g_{\text{eff}}^2 = 4\pi$  to account for the fact that the interaction would become strong at  $\sqrt{s} \simeq \Lambda$  and, by convention,  $|\eta_{ij}| = \pm 1$  or  $\eta_{ij} = 0$ . This leaves the energy scales  $\Lambda_{ij}$  as free, *a priori* independent parameters.

Clearly, at  $s \ll \Lambda_{ij}^2$ , the Lagrangian (1) can only contribute virtual effects, to be sought-for as very small deviations of the measured observables from the Standard Model (SM) predictions. The relative size of such effects is expected to be of order  $s/\alpha\Lambda^2$ , with  $\alpha$  the SM coupling (essentially, the fine structure constant) and, therefore, very high collider energies and luminosities are required for this kind of searches. In practice, the constraints and the attainable reach on the CI couplings can be numerically assessed by comparing the theoretical deviations with the foreseen experimental uncertainties on the cross sections.

For the case of the Bhabha process (2), the effective Lagrangian  $\mathcal{L}_{\text{CI}}$  in Eq. (1) envisages the existence of six individual, and independent, CI models, contributing to individual helicity amplitudes or combinations of them with *a priori* free, and nonvanishing, coefficients

(basically,  $\epsilon_{LL}, \epsilon_{RR}$  and  $\epsilon_{LR}$  combined with the  $\pm$  signs). Correspondingly, in principle the most general, and model-independent, analysis of the data must account for the situation where all four-fermion effective couplings defined in Eq. (1) are simultaneously allowed in the expression for the cross section. Potentially, the different CI couplings may interfere and substantially weaken the bounds. Indeed, although the different helicity amplitudes by themselves do not interfere, *the deviations from the SM* could be positive for one helicity amplitude and negative for another, so that accidental cancellation might occur in the sought-for deviations from the SM predictions for the relevant observables.

The simplest attitude is to assume non-zero values for only one of the couplings (or one specific combination of them) at a time, with all others zero, and this leads to tests of the specific models mentioned above. Also, in many cases, global analyses combining data from different experiments relevant to the considered type of coupling are performed. Current lower bounds on the corresponding  $\Lambda$ 's obtained along this line from recent analyses of  $e^+e^- \rightarrow \bar{f}f$  at LEP, that include Bhabha scattering, are in the range 8-20 TeV and are found to substantially depend on the considered one-parameter scenario [3, 4]. Examples of results for the  $eeff$  couplings for the different fermion species in (1), from analyses of different kinds of processes and experiments, can be found, *e.g.*, in Refs. [5–9].

It should be highly desirable to apply a more general (and model-independent) approach to the analysis of the experimental data, that allows to simultaneously include all terms of Eq. (1) as independent, non vanishing free parameters, and yet to derive separate constraints (or exclusion regions) on the values of the CI coupling constants, free from potential weakening due to accidental cancellations.

Such an analysis is feasible with initial beam longitudinal polarization, a possibility envisaged at the LC [10]. This allows to extract the individual helicity cross sections from suitable combinations of measurable polarized cross sections and, consequently, to disentangle the constraints on the corresponding CI constants  $\epsilon_{ij}$ , *see, e.g.*, Refs. [11–18]. In what follows, we wish to complement the model-independent analysis of  $e^+e^- \rightarrow \bar{f}f$  with  $f \neq e, t$  given in Refs. [17, 18], with a discussion of the role of the polarized differential cross sections measurable at the LC in the derivation of model-independent bounds on the three independent four-electron contact interactions relevant to the Bhabha process (2).<sup>1</sup>

Specifically, in Sect. 2 we introduce the observables being considered, and in Sect. 3 we present a numerical analysis and the assessment of the attainable reach on the CI couplings, resulting from a  $\chi^2$  procedure that accounts for the expected experimental uncertainties (statistical and systematical ones). Finally, Sect. 4 contains a comparison with the results previously obtained for  $e^+e^- \rightarrow \mu^+\mu^-$  and some conclusive remarks.

## 2 Polarized observables

With  $P^-$  and  $P^+$  the longitudinal polarization of the electron and positron beams, respectively, and  $\theta$  the angle between the incoming and the outgoing electrons in the c.m. frame,

---

<sup>1</sup>Notice that, in general, for  $e^+e^- \rightarrow \bar{f}f$  with  $f \neq e$  there are four independent CI couplings, apart from the  $\pm$  possibility, so that in the present case of process (2) there is one free parameter less.

the differential cross section of process (2) at lowest order, including  $\gamma$  and  $Z$  exchanges both in the  $s$  and  $t$  channels and the contact interaction (1), can be written in the following form [11, 12, 15]:

$$\frac{d\sigma(P^-, P^+)}{d\cos\theta} = (1 - P^- P^+) \frac{d\sigma_1}{d\cos\theta} + (1 + P^- P^+) \frac{d\sigma_2}{d\cos\theta} + (P^+ - P^-) \frac{d\sigma_P}{d\cos\theta}. \quad (3)$$

In Eq. (3):

$$\begin{aligned} \frac{d\sigma_1}{d\cos\theta} &= \frac{\pi\alpha^2}{4s} [A_+(1 + \cos\theta)^2 + A_-(1 - \cos\theta)^2], \\ \frac{d\sigma_2}{d\cos\theta} &= \frac{\pi\alpha^2}{4s} 4A_0, \\ \frac{d\sigma_P}{d\cos\theta} &= \frac{\pi\alpha^2}{4s} A_+^P (1 + \cos\theta)^2, \end{aligned} \quad (4)$$

with

$$\begin{aligned} A_0(s, t) &= \left(\frac{s}{t}\right)^2 \left|1 + g_R g_L \chi_Z(t) + \frac{t}{\alpha} \epsilon_{LR}\right|^2, \\ A_+(s, t) &= \frac{1}{2} \left|1 + \frac{s}{t} + g_L^2 \left(\chi_Z(s) + \frac{s}{t} \chi_Z(t)\right) + 2\frac{s}{\alpha} \epsilon_{LL}\right|^2 \\ &\quad + \frac{1}{2} \left|1 + \frac{s}{t} + g_R^2 \left(\chi_Z(s) + \frac{s}{t} \chi_Z(t)\right) + 2\frac{s}{\alpha} \epsilon_{RR}\right|^2, \\ A_-(s, t) &= \left|1 + g_R g_L \chi_Z(s) + \frac{s}{\alpha} \epsilon_{LR}\right|^2, \\ A_+^P(s, t) &= \frac{1}{2} \left|1 + \frac{s}{t} + g_L^2 \left(\chi_Z(s) + \frac{s}{t} \chi_Z(t)\right) + 2\frac{s}{\alpha} \epsilon_{LL}\right|^2 \\ &\quad - \frac{1}{2} \left|1 + \frac{s}{t} + g_R^2 \left(\chi_Z(s) + \frac{s}{t} \chi_Z(t)\right) + 2\frac{s}{\alpha} \epsilon_{RR}\right|^2. \end{aligned} \quad (5)$$

Here:  $\alpha$  is the fine structure constant;  $t = -s(1 - \cos\theta)/2$  and  $\chi_Z(s) = s/(s - M_Z^2 + iM_Z\Gamma_Z)$ ,  $\chi_Z(t) = t/(t - M_Z^2)$  represent the  $Z$  propagator in the  $s$  and  $t$  channels, respectively, with  $M_Z$  and  $\Gamma_Z$  the mass and width of the  $Z$ ;  $g_R = \tan\theta_W$ ,  $g_L = -\cot 2\theta_W$  are the SM right- and left-handed electron couplings of the  $Z$ , with  $\theta_W$  the electroweak mixing angle.

With both beams polarized, the polarization of each beam can be changed on a pulse by pulse basis. This would allow the separate measurement of the polarized cross sections for each of the four polarization configurations  $++$ ,  $--$ ,  $+-$  and  $-+$ , corresponding to the four sets of beam polarizations  $(P^-, P^+) = (P_1, P_2)$ ,  $(-P_1, -P_2)$ ,  $(P_1, -P_2)$  and  $(-P_1, P_2)$ , respectively, with  $0 < P_{1,2} < 1$ . Specifically, with the simplifying notation  $d\sigma \equiv d\sigma/d\cos\theta$ :

$$\begin{aligned} d\sigma_{++} &\equiv d\sigma(P_1, P_2) = (1 - P_1 P_2) d\sigma_1 + (1 + P_1 P_2) d\sigma_2 + (P_2 - P_1) d\sigma_P, \\ d\sigma_{--} &\equiv d\sigma(-P_1, -P_2) = (1 - P_1 P_2) d\sigma_1 + (1 + P_1 P_2) d\sigma_2 - (P_2 - P_1) d\sigma_P, \\ d\sigma_{+-} &\equiv d\sigma(P_1, -P_2) = (1 + P_1 P_2) d\sigma_1 + (1 - P_1 P_2) d\sigma_2 - (P_2 + P_1) d\sigma_P, \\ d\sigma_{-+} &\equiv d\sigma(-P_1, P_2) = (1 + P_1 P_2) d\sigma_1 + (1 - P_1 P_2) d\sigma_2 + (P_2 + P_1) d\sigma_P. \end{aligned} \quad (6)$$

To extract from the measured polarized cross sections the values of  $d\sigma_1$ ,  $d\sigma_2$  and  $d\sigma_P$ , that carry the information on the CI couplings, one has to invert the system of equations (6). The solution reads:

$$\begin{aligned} d\sigma_1 &= \frac{1}{8} \left[ \left(1 - \frac{1}{P_1 P_2}\right) (d\sigma_{++} + d\sigma_{--}) + \left(1 + \frac{1}{P_1 P_2}\right) (d\sigma_{+-} + d\sigma_{-+}) \right], \\ d\sigma_2 &= \frac{1}{8} \left[ \left(1 + \frac{1}{P_1 P_2}\right) (d\sigma_{++} + d\sigma_{--}) + \left(1 - \frac{1}{P_1 P_2}\right) (d\sigma_{+-} + d\sigma_{-+}) \right], \\ d\sigma_P &= -\frac{1}{2(P_1 + P_2)} (d\sigma_{+-} - d\sigma_{-+}) = \frac{1}{2(P_2 - P_1)} (d\sigma_{++} - d\sigma_{--}). \end{aligned} \quad (7)$$

Notice that the equations in (6) are not all linearly independent, and that not only  $P_1 \neq 0$  and  $P_2 \neq 0$ , but also  $P_1 \neq P_2$  is needed to obtain  $d\sigma_P$  *via*  $d\sigma_{++}$  and  $d\sigma_{--}$ . As one can see from Eqs.(4) and (5),  $\sigma_2$  depends on only one contact interaction parameter ( $\epsilon_{LR}$ ),  $\sigma_P$  is two-parameter dependent ( $\epsilon_{RR}$  and  $\epsilon_{LL}$ ), and  $\sigma_1$  depends on all three parameters. Therefore, the derivation of the model-independent constraints on the CI couplings requires the combination of all polarized observables of Eq. (6). In this regard, to emphasize the role of polarization, one can observe from Eqs. (3)-(5) that, in the unpolarized case  $P_1 = P_2 = 0$  where only  $\sigma_1$  and  $\sigma_2$  appear, the interference of the  $\epsilon_{LR}$  term with the SM amplitude in  $A_0$  and  $A_-$  has opposite signs, leading to a partial cancellation for  $-t \sim s$ . Consequently, as anticipated in Sect. 1, one expects the unpolarized cross section to have reduced sensitivity to  $\epsilon_{LR}$ . Conversely,  $\epsilon_{LR}$  is *directly* accessible from  $d\sigma_2$ , *via* polarized cross sections as in Eq. (7). Also, considering that numerically  $g_L^2 \cong g_R^2$ , the parameters  $\epsilon_{LL}$  and  $\epsilon_{RR}$  contribute to the unpolarized cross section through  $A_+$  with equal coefficients, so that, in general, only correlations of the form  $|\epsilon_{LL} + \epsilon_{RR}| < \text{const}$ , and not finite allowed regions, could be derived in this case.

To make contact to the experiment we take  $P_1 = 0.8$  and  $P_2 = 0.6$ , and impose a cut in the forward and backward directions. Specifically, we consider the cut angular range  $|\cos \theta| < 0.9$  and divide it into nine equal-size bins of width  $\Delta z = 0.2$  ( $z \equiv \cos \theta$ ). We also introduce the experimental efficiency,  $\epsilon$ , for detecting the final  $e^+e^-$  pair and, according to the LEP2 experience,  $\epsilon = 0.9$  is assumed.

We then define the four, directly measurable, event rates integrated over each bin:

$$N_{++}, \quad N_{--}, \quad N_{+-}, \quad N_{-+}, \quad (8)$$

and ( $\alpha\beta = ++$ , etc.):

$$N_{\alpha\beta}^{\text{bin}} = \frac{1}{4} \mathcal{L}_{\text{int}} \epsilon \int_{\text{bin}} (d\sigma_{\alpha\beta}/dz) dz. \quad (9)$$

In Eq. (9),  $\mathcal{L}_{\text{int}}$  is the time-integrated luminosity, which is assumed to be equally divided among the four combinations of electron and positron beams polarization defined in Eqs. (6).

In Fig. 1, the bin-integrated angular distributions of  $N_{++}^{\text{bin}}$  and  $N_{+-}^{\text{bin}}$  in the SM at  $\sqrt{s} = 500$  GeV and  $\mathcal{L}_{\text{int}} = 50 \text{ fb}^{-1}$  are presented as histograms. Here, the SM cross sections have

been evaluated by means of the effective Born approximation [19, 20]. The typical forward peak, dominated by the  $t$ -channel photon pole, dramatically shows up, and determines a really large statistics available in the region of small  $t$ . The  $\cos\theta$  distributions for the other polarization configurations in (6) are similar and, therefore, we do not represent them here.

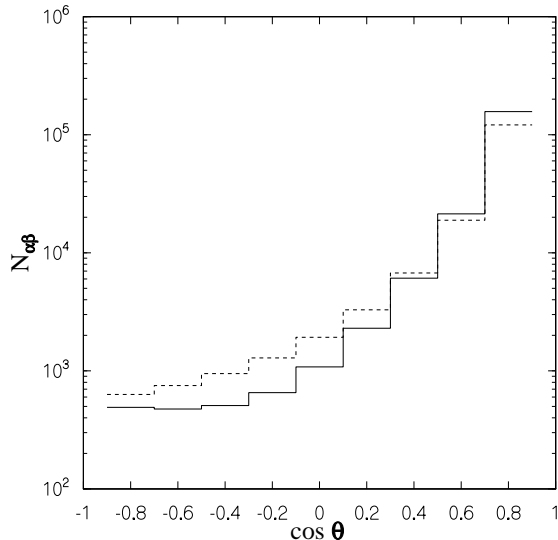


Figure 1: Bin-integrated angular distributions of  $N_{+-}^{\text{bin}}$  (solid line) and  $N_{++}^{\text{bin}}$  (dashed line), Eq.(9), in the SM at  $\sqrt{s} = 500$  GeV and  $\mathcal{L}_{\text{int}} = 50 \text{ fb}^{-1}$ .

The next step is to define the relative deviations of the cross sections  $\sigma_1$ ,  $\sigma_2$  and  $\sigma_P$  from the SM predictions, due to the contact interaction. In general, for such deviations, we use the notation:

$$\Delta_{\mathcal{O}} = \frac{\mathcal{O}(SM + CI) - \mathcal{O}(SM)}{\mathcal{O}(SM)}, \quad (10)$$

To get an illustration of the effect of the contact interactions on the observables (7) under consideration, we show in Fig. 2a and Fig. 2b the angular distributions of the relative deviations of  $d\sigma_1$  and  $d\sigma_2$ , taking as examples the values of  $\mathcal{L}_{\text{int}}$  and  $\Lambda_{ij}$  indicated in the captions. The SM predictions are evaluated in the same, effective Born, approximation as in Fig. 1. The deviations are then compared to the expected statistical uncertainties, represented by the vertical bars. Fig. 2a shows that  $d\sigma_1$  is sensitive to contact interactions in the forward region, where the ratio of the ‘signal’ to the statistical uncertainty increases. Also, it indicates that, for the chosen values of the c.m. energy  $\sqrt{s}$  and  $\mathcal{L}_{\text{int}}$ , the reach on  $\Lambda_{ij}$  will be substantially larger than 30 TeV. Conversely, Fig. 2b shows that the sensitivity of  $d\sigma_2$  is almost independent on the chosen kinematical range in  $\cos\theta$ , leading to a really high sensitivity of this observable to  $\epsilon_{\text{LR}}$ , and to corresponding lower bounds on  $\Lambda_{\text{LR}}$  potentially

larger than 50 TeV. We now proceed to the analysis of the bounds on the contact interaction couplings.

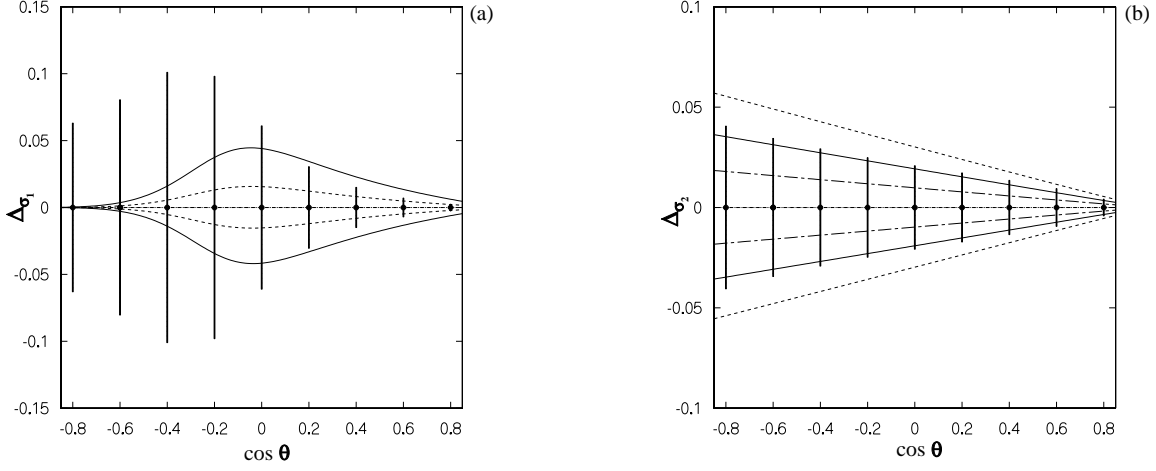


Figure 2: The angular distributions for the relative deviations  $\Delta_{\sigma_1}$  (a) at  $\Lambda_{RR}=30$  TeV (solid line) and 50 TeV (dashed line), and for  $\Delta_{\sigma_2}$  (b) at  $\Lambda_{LR}=40$  TeV (dashed line), 50 TeV (solid line), 70 TeV (dot-dashed line). The curves above (below) the horizontal line correspond to negative (positive) interference between contact interaction and SM amplitude. The error bars show the expected statistical error at  $\mathcal{L}_{\text{int}} = 50 \text{ fb}^{-1}$ .

### 3 Numerical analysis and constraints on CI couplings

To assess the sensitivity to the compositeness scale we assume the data to be well described by the SM predictions ( $\epsilon_{ij} = 0$ ), *i.e.*, that no deviation is observed within the foreseen experimental accuracy, and perform a  $\chi^2$  analysis of the  $\cos\theta$  angular distribution. For each of the observable cross sections, the  $\chi^2$  distribution is defined as the sum over the above mentioned nine equal-size  $\cos\theta$  bins:

$$\chi^2(\mathcal{O}) = \sum_{\text{bins}} \left( \frac{\Delta\mathcal{O}^{\text{bin}}}{\delta\mathcal{O}^{\text{bin}}} \right)^2, \quad (11)$$

where  $\mathcal{O} = \sigma_1, \sigma_2, \sigma_P$  and  $\sigma^{\text{bin}} \equiv \int_{\text{bin}} (d\sigma/dz) dz$ . In Eq. (11),  $\Delta\mathcal{O}$  represents the deviation from the SM prediction,  $\Delta\mathcal{O} = \mathcal{O}(SM + CI) - \mathcal{O}(SM)$ , which can be easily expressed in terms of the CI couplings by using Eqs. (5), and  $\delta\mathcal{O}$  is the expected experimental uncertainty, that combines the statistical and the systematic ones.

In the following analysis, the theoretical expectations for the polarized cross sections are evaluated by using the program TOPAZ0 [21, 22], adapted to the present discussion, with  $m_{\text{top}} = 175$  GeV and  $M_H = 120$  GeV. For electron-positron final states, a cut on

the acollinearity angle between electron and positron,  $\theta_{\text{acol}} < 10^\circ$ , is applied to select non-radiative events.

Concerning the numerical inputs and assumptions used in the estimate of  $\delta\mathcal{O}$ , to assess the role of statistics we vary  $\mathcal{L}_{\text{int}}$  from 50 to 500 fb $^{-1}$  (a quarter of the total running time for each polarization configuration). As for the systematic uncertainty, we take  $\delta\mathcal{L}_{\text{int}}/\mathcal{L}_{\text{int}} = 0.5\%$ ,  $\delta\epsilon/\epsilon = 0.5\%$  and, regarding the electron and positron degrees of polarization,  $\delta P_1/P_1 = \delta P_2/P_2 = 0.5\%$ .

For example, in the case of  $\sigma_2$ , the deviation from the SM prediction, largely dominated for  $\sqrt{s} \ll \Lambda_{\text{LR}}$  by the interference term, can be represented as:

$$\Delta\sigma_2^{\text{bin}} \equiv \sigma_2^{\text{bin}}(SM + CI) - \sigma_2^{\text{bin}}(SM) \simeq 2\pi\alpha s\epsilon_{\text{LR}} \int_{\text{bin}} \frac{d\cos\theta}{t} (1 + g_R g_L \chi_Z(t)), \quad (12)$$

and, combining uncertainties in quadrature, the uncertainty on  $\sigma_2$ , indirectly determined *via* the measured  $\sigma_{++}$ ,  $\sigma_{--}$ ,  $\sigma_{+-}$  and  $\sigma_{-+}$  as in Eq. (7), can be expressed as

$$(\delta\sigma_2)^2 = \frac{1}{8^2} \left[ \left(1 + \frac{1}{P_1 P_2}\right)^2 ((\delta\sigma_{++})^2 + (\delta\sigma_{--})^2) + \left(1 - \frac{1}{P_1 P_2}\right)^2 ((\delta\sigma_{+-})^2 + (\delta\sigma_{-+})^2) \right] \\ + \left( \frac{\sigma_{++} + \sigma_{--} - \sigma_{+-} - \sigma_{-+}}{8P_1 P_2} \right)^2 \left[ \left(\frac{\delta P_1}{P_1}\right)^2 + \left(\frac{\delta P_2}{P_2}\right)^2 \right], \quad (13)$$

with

$$\left( \frac{\delta\sigma_{\alpha\beta}}{\sigma_{\alpha\beta}} \right)^2 = \frac{1}{N_{\alpha\beta}} + \left( \frac{\delta\mathcal{L}_{\text{int}}}{\mathcal{L}_{\text{int}}} \right)^2 + \left( \frac{\delta\epsilon}{\epsilon} \right)^2. \quad (14)$$

Analogous expressions hold for the uncertainties relevant to  $\sigma_1$  and  $\sigma_P$ .

As a criterion to constrain the allowed values of the contact interaction parameters by the non-observation of the corresponding deviations, we impose  $\chi^2 < \chi_{\text{CL}}^2$ , where the actual value of  $\chi_{\text{CL}}^2$  specifies the desired ‘confidence’ level. We take the values  $\chi_{\text{CL}}^2 = 3.84$  and 5.99 for 95% C.L. for a one- and a two-parameter fit, respectively.

We begin with the presentation of the numerical results for  $\epsilon_{\text{LR}}$ . In this case, the relevant cross section  $\sigma_2$  depends on  $\epsilon_{\text{LR}}$  only, see Eqs. (4) and (5) and, therefore, the constraints on that parameter are determined from a one-parameter fit. The model-independent, discovery reach expected at the LC for the corresponding mass scale  $\Lambda_{\text{LR}}$  is represented, as a function of the integrated luminosity  $\mathcal{L}_{\text{int}}$ , by the solid line in Fig. 3. As expected, the highest luminosity determines the strongest constraints on the CI couplings.<sup>2</sup> Fig. 3 dramatically shows the really high sensitivity of  $\sigma_2$ , such that the discovery limits on  $\Lambda_{\text{LR}}$  are the highest, compared to the  $\Lambda_{\text{RR}}$  and  $\Lambda_{\text{LL}}$  cases, and can be as large as 110 up to 170 times the total c.m. energy. Actually, the  $\Lambda_{\text{LR}}$  limits are large enough that the approximation used in Eq. (12) is good for all values of  $t$ , so that the derived limits are independent of the sign of the  $\epsilon_{\text{LR}}$ .

---

<sup>2</sup>Such increase with luminosity is somewhat slower than expected from the scaling law  $\Lambda \sim (s\mathcal{L}_{\text{int}})^{1/4}$ , as the effect of the systematic uncertainties competing with the statistical ones.



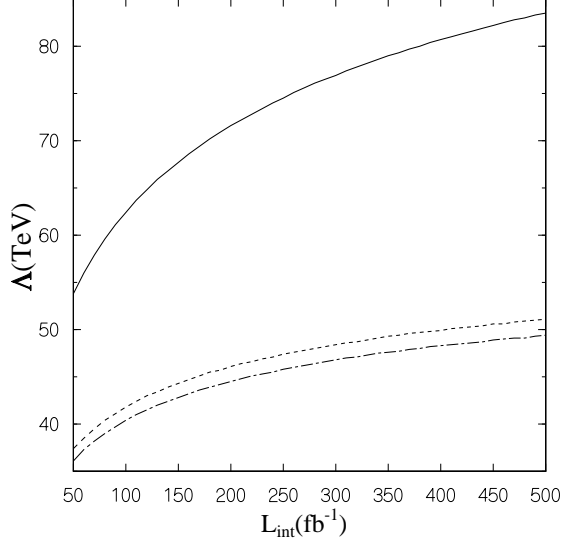


Figure 3: Reach in  $\Lambda_{ij}$  at 95% C.L. *vs.* integrated luminosity  $\mathcal{L}_{\text{int}}$  obtained from the model-independent analysis for  $e^+ + e^- \rightarrow e^+ + e^-$  at  $\sqrt{s} = 0.5$  TeV,  $|P^-| = 0.8$  and  $|P^+| = 0.6$ ,  $\Lambda_{\text{LR}}$  (solid line),  $\Lambda_{\text{LL}}$  (dashed line),  $\Lambda_{\text{RR}}$  (dot-dash line).

Since  $\sigma_P$  simultaneously depends on the two independent CI couplings  $\epsilon_{\text{RR}}$  and  $\epsilon_{\text{LL}}$ , a two-parameter analysis is needed in this case. Here, the terms quadratic in  $\epsilon_{\text{LL}}$  and  $\epsilon_{\text{RR}}$  largely cancel leaving the remaining interference to dominate the relevant deviations from the SM, and consequently the resulting constraint has the form of a straight band, as depicted in Fig. 4a. Indeed, such a band represents a correlation between the two parameters, rather than a bound around the SM value  $\epsilon_{\text{LL}} = \epsilon_{\text{RR}} = 0$ .

In order to get a restricted allowed region around zero, one can combine the above mentioned band with the exclusion region obtained from  $\sigma_1$ . However, since the latter depends on *all three* contact interaction parameters, see Eqs. (4) and (5), to set constraints in the  $(\epsilon_{\text{RR}}, \epsilon_{\text{LL}})$  plane requires the combination of the  $\sigma_1$ -bounds with the limits on  $\epsilon_{\text{LR}}$  derived above from  $\sigma_2$ . The bound in the  $(\epsilon_{\text{RR}}, \epsilon_{\text{LL}})$  resulting from this procedure is shown in Fig. 4a and, finally, the shaded ellipse determined by the combination with the band determined by  $\sigma_P$  represents the restricted allowed region around the SM point  $\epsilon_{ij} = 0$ . With reference to Eq. (11), for the  $\chi^2$  analysis this amounts to the consideration of the combined  $\chi^2(\sigma_1) + \chi^2(\sigma_P)$ . Fig. 4b is essentially a magnification of the shaded region of Fig. 4a, and represents the model-independent limits on  $\epsilon_{\text{LL}}$  and  $\epsilon_{\text{RR}}$  attainable at the considered LC, for two possible values of the integrated luminosity. These bounds are translated into the model-independent reach on the mass scale parameters  $\Lambda_{\text{LL}}$  and  $\Lambda_{\text{RR}}$ , represented as a function of luminosity in Fig. 3. The fact that such bounds are substantially lower than those for  $\Lambda_{\text{LR}}$  reflects that a combined two-parameter  $\chi^2$  analysis must be used. In this regard, the calculation presented here indicates that not only polarization,

but also combinations of measurements of polarized observables are necessary to obtain model-independent bounds on the CI couplings.

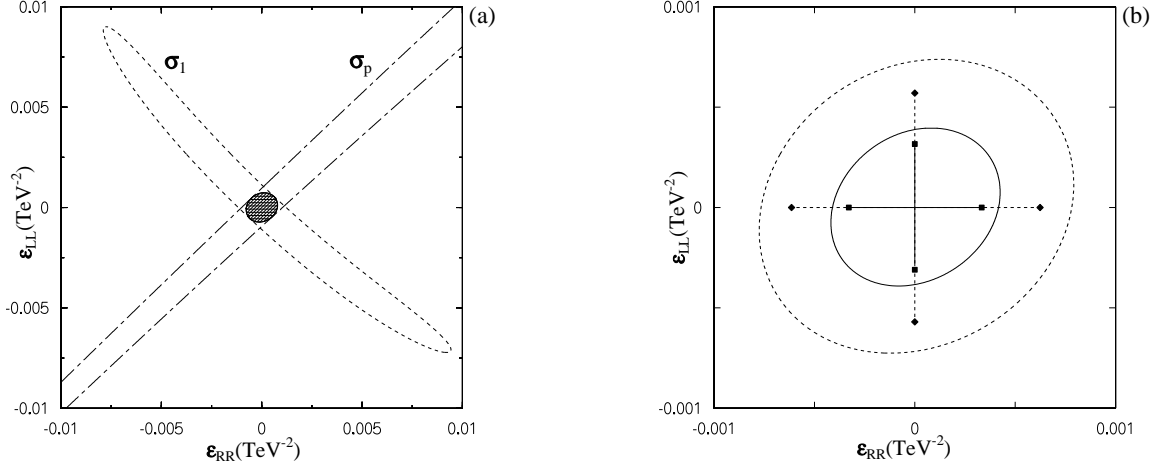


Figure 4: (a) Allowed areas at 95% C.L. on electron contact interaction parameters in the planes  $(\epsilon_{RR}, \epsilon_{LL})$ , obtained from  $\sigma_1$  and  $\sigma_P$  at  $\sqrt{s} = 500$  GeV and  $\mathcal{L}_{\text{int}} = 50 \text{ fb}^{-1}$  (a); (b) Combined allowed regions at 95% C.L. obtained from  $\sigma_1$  and  $\sigma_P$  at  $\sqrt{s} = 500$  GeV,  $\mathcal{L}_{\text{int}} = 50 \text{ fb}^{-1}$  (outer ellipse) and  $500 \text{ fb}^{-1}$  (inner ellipse).

The crosses in Fig. 4b represent the model-dependent constraints obtainable by taking only one non-zero parameter at a time, either  $\epsilon_{LL}$  or  $\epsilon_{RR}$ , instead of the two simultaneously non-zero and independent as in the analysis discussed above. Similar to the inner and outer ellipses, the shorter and longer arms of the crosses refer to integrated luminosity  $\mathcal{L}_{\text{int}} = 50 \text{ fb}^{-1}$  and  $500 \text{ fb}^{-1}$ , respectively. One can note from Fig. 4b that the ‘single-parameter’ constraints on the individual CI parameters  $\epsilon_{RR}$  and  $\epsilon_{LL}$  are numerically more stringent, as compared to the model-independent ones. Essentially, this is a reflection of the smaller value of the critical  $\chi^2$ ,  $\chi_{\text{CL}}^2 = 3.84$  corresponding to 95% C.L. with a *one-parameter* fit.

## 4 Concluding remarks

In the previous sections we have derived limits on the contact interactions relevant to Bhabha scattering by a model-independent analysis that allows to simultaneously account for all independent couplings as non-vanishing free parameters. The results for the lower bounds on the corresponding mass scales  $\Lambda$  range, depending on the luminosity, from essentially 38 to 50 TeV for the LL and RR cases, and from 54 to 84 TeV for the LR case. The comparison with the numerical results relevant to the  $e^+e^- \rightarrow \mu^+\mu^-$  channel, derived from a similar analysis [18], is shown in Table 1.

The table shows that for  $\Lambda_{LL}$  and  $\Lambda_{RR}$  the restrictions from  $e^+e^- \rightarrow \mu^+\mu^-$  and  $e^+e^- \rightarrow e^+e^-$  are qualitatively comparable. Instead, the sensitivity to  $\Lambda_{LR}$ , and the corresponding

Table 1: Reach in  $\Lambda_{ij}$  at 95% C.L., from the model-independent analysis performed for  $e^+e^- \rightarrow \mu^+\mu^-$  and  $e^+e^-$ , at  $E_{\text{c.m.}} = 0.5$  TeV,  $\mathcal{L}_{\text{int}} = 50 \text{ fb}^{-1}$  and  $500 \text{ fb}^{-1}$ ,  $|P^-| = 0.8$  and  $|P^+| = 0.6$ .

process	$\mathcal{L}_{\text{int}}$ $\text{fb}^{-1}$	$\Lambda_{\text{LL}}$ TeV	$\Lambda_{\text{RR}}$ TeV	$\Lambda_{\text{LR}}$ TeV	$\Lambda_{\text{RL}}$ TeV
$e^+e^- \rightarrow \mu^+\mu^-$	50	35	35	31	31
	500	47	49	51	52
$e^+e^- \rightarrow e^+e^-$	50	38	36	54	
	500	51	49	84	

lower bound, is dramatically higher in the case of Bhabha scattering. In this regard, this is the consequence of the initial beams longitudinal polarization that allows, by measuring suitable combinations of polarized cross sections, to directly disentangle the coupling  $\epsilon_{\text{LR}}$ . Indeed, as previously observed, in general without polarization only correlations among couplings, rather than finite allowed regions, could be derived or, alternatively, a one-parameter analysis testing individual models can be performed.

As an example of application of the obtained results to a possible source of contact interactions, we may consider the sneutrino parameters (mass  $m_{\tilde{\nu}}$  and Yukawa coupling  $\lambda$ ) envisaged by supersymmetric theories with  $\mathcal{R}$ -parity breaking. In this case, sneutrino exchange affects only those helicity amplitudes with non-diagonal chiral indices, so that  $\Lambda_{\text{LR}}$  is the relevant mass scale [23, 24]. Qualitatively, without entering into a detailed and more complex analysis, one can expect typical bounds on  $m_{\tilde{\nu}}/\lambda \sim \Lambda_{\text{LR}}/\sqrt{8\pi} \simeq 11$  to 17 TeV corresponding to  $\Lambda_{\text{LR}} \approx 54$  TeV and 84 TeV (Fig. 3) at  $\mathcal{L}_{\text{int}} = 50 \text{ fb}^{-1}$  and  $500 \text{ fb}^{-1}$ , respectively.

### Acknowledgements

This research has been partially supported by MURST (Italian Ministry of University, Scientific Research and Technology) and by funds of the University of Trieste.

## References

- [1] G. 't Hooft, in *Recent Developments in Gauge Theories*, eds. G. 't Hooft et al., Plenum, New York (1980).
- [2] E. Eichten, K. Lane and M. E. Peskin, Phys. Rev. Lett. **50** (1983) 811;  
R. Rückl, Phys. Lett. B **129** (1983) 363;  
E. Eichten, I. Hinchliffe, K. Lane and C. Quigg, Rev. Mod. Phys. **56** (1984) 579;  
and references there.
- [3] D. Abbaneo *et al.* [ALEPH Collaboration], CERN-EP-2000-016.

- [4] D. Bourilkov, hep-ph/0104165.
- [5] V. Barger, K. Cheung, K. Hagiwara and D. Zeppenfeld, Phys. Rev. D **57** (1998) 391 [hep-ph/9707412];  
D. Zeppenfeld and K. Cheung, hep-ph/9810277;  
K. Cheung, hep-ph/0106251.
- [6] G. Altarelli, J. Ellis, G. F. Giudice, S. Lola and M. L. Mangano, Nucl. Phys. B **506** (1997) 3 [hep-ph/9703276];  
R. Casalbuoni, S. De Curtis, D. Dominici and R. Gatto, Phys. Lett. B **460** (1999) 135 [hep-ph/9905568].
- [7] A. F. Zarnecki, Eur. Phys. J. C **11** (1999) 539 [hep-ph/9904334].
- [8] A. F. Zarnecki, Nucl. Phys. Proc. Suppl. **79** (1999) 158 [hep-ph/9905565].
- [9] V. Barger and K. Cheung, Phys. Lett. B **480** (2000) 149 [hep-ph/0002259].
- [10] See, *e.g.*: J. A. Aguilar-Saavedra *et al.*, DESY-2001-011 [hep-ph/0106315].
- [11] B. Schrempp, F. Schrempp, N. Wermes and D. Zeppenfeld, Nucl. Phys. B **296** (1988) 1.
- [12] D. Bardin, W. Hollik and T. Riemann, Z. Phys. C **49** (1991) 485.
- [13] T. L. Barklow, Int. J. Mod. Phys. A **11** (1996) 1579.
- [14] E. J. Eichten and S. Keller, in *Batavia 1997: Physics at the first muon collider*, FERMILAB-CONF-98-011-T (1998) [hep-ph/9801258].
- [15] M. Beccaria, F. M. Renard, S. Spagnolo and C. Verzegnassi, Phys. Rev. D **62** (2000) 053003 [hep-ph/000210].
- [16] S. Riemann, LC Note LC-TH-2001-007 (2001).
- [17] A. A. Babich, P. Osland, A. A. Pankov and N. Paver, Phys. Lett. B **476** (2000) 95 [hep-ph/9910403]; Phys. Lett. B **481** (2000) 263 [hep-ph/0003253]; LC Note LC-TH-2001-021 (2001) [hep-ph/0101150].
- [18] A. A. Babich, P. Osland, A. A. Pankov and N. Paver, hep-ph/0107159, to appear in Phys. Lett. B.
- [19] M. Consoli, W. Hollik and F. Jegerlehner, CERN-TH-5527-89 *Presented at Workshop on Z Physics at LEP*.
- [20] G. Altarelli, R. Casalbuoni, D. Dominici, F. Feruglio and R. Gatto, Nucl. Phys. B **342** (1990) 15.

- [21] G. Montagna, F. Piccinini, O. Nicrosini, G. Passarino and R. Pittau, Nucl. Phys. B **401** (1993) 3.
- [22] G. Montagna, O. Nicrosini, F. Piccinini and G. Passarino, Comput. Phys. Commun. **76** (1993) 328; Comput. Phys. Commun. **117** (1999) 278 [hep-ph/9804211].
- [23] T. G. Rizzo, Phys. Rev. D **59** (1999) 113004 [hep-ph/9811440].
- [24] J. Kalinowski, R. Rückl, H. Spiesberger and P. M. Zerwas, Phys. Lett. B **406** (1997) 314 [hep-ph/9703436].